Article

Not peer-reviewed version

Investigating Potential 5’ UTR G-Quadruplexes Within NRF2 mRNA

Hatice Esenkaya * and Joe Bryant

Posted Date: 21 January 2026

doi: 10.20944/preprints202601.1129.v1

Keywords: nuclear factor erythroid 2 related factor; pyridostatin; RNA-binding proteins; G-quadruplexes; 5’ untranslated regions; cancer

 doi:10.20944/preprints202601.1129.v1

Article

Investigating Potential 5′ UTR G-Quadruplexes Within NRF2 mRNA

Hatice Esenkaya [1,2] * and Joe Bryant [3]

[1] Kilis 7 Aralık University, Sweden
[2] Karolinska Institutet, Sweden
[3] University of Surrey, UK
* Correspondence: hatice.esenkaya@kilis.edu.tr (H.E.)

Abstract

Post-transcriptional regulation of gene expression is influenced by RNA-binding proteins (RBPs) and small non-coding RNAs which bind to conserved mRNA sequences to modulate mRNA processing. These regulatory molecules effect the structural conformation of mRNAs, creating formations like G-quadruplexes (G4s) which alter translation initiation and regulatory factor site accessibility. Recent studies have highlighted Nuclear factor erythroid 2-related factor 2 (NRF2) as a key regulator of cellular redox homeostasis and cellular response to oxidative stress. An intriguing feature of NRF2 is the structural formation of its 5′ untranslated region (UTR) which may promote or inhibit translation initiation depending on the cellular context. In this study with mini genes, we provide evidence of RNA G4s in NRF2 mRNA's 5′ UTR regions under basal (no stress) conditions in vitro through EMSA and fluorescence spectra in the presence of pyridostatin. Understanding how structural motifs within NRF2's 5′UTR regions influence mRNA function provides insights into a common molecular mechanism underlying diseases where NRF2 is dysregulated, like cancers, cardiovascular disease, and neurodegeneration, and highlights potential therapeutic avenues through regulation of NRF2.

Keywords: nuclear factor erythroid 2 related factor; pyridostatin; RNA-binding proteins; G-quadruplexes; 5′ untranslated regions; cancer

1. Introduction

The regulation of gene expression is a complex and finely tuned process, with messenger RNA (mRNA) playing a crucial intermediary role between DNA and protein synthesis (1). The structure of mRNA (2), including its 5′ untranslated region (UTR) (3), 3′ UTR (4), and coding region (5), is pivotal in determining the efficiency and timing of gene expression (6). While the coding region contains the information for protein synthesis (7), the 5′ and 3′ UTRs serve as key regulatory regions that influence mRNA stability (8), translation initiation (9), and post-transcriptional modifications (10). The 5′ UTR, located upstream of the coding sequence (11), is particularly important for regulating the initiation of translation (12), and often harbours elements like secondary structures (3), upstream open reading frames (uORFs) (13), and binding sites for regulatory proteins or small RNAs (14). Meanwhile, the downstream 3′ UTR typically influences an mRNA's: stability (15), intracellular localisation (16), and degradation through elements like microRNA binding sites (17), or polyadenylation signals (18). Together these regions contribute to a dynamic regulation of gene expression that allows cells to adapt rapidly to changing conditions (19), coordinating the production of proteins essential for cellular function and survival. Understanding the features of UTR's that facilitate post-transcriptional gene regulation will provide valuable insights into their potential implications in diseases during which these processes are often dysregulated, such as cancer (20) or neurological disorders (21).

The Nuclear Factor Erythroid 2 Related Factor 2 (NRF2) gene plays a crucial role in maintaining cellular homeostasis by regulating several key signalling pathways including the antioxidant

 doi:10.20944/preprints202601.1129.v1

response (22), detoxification processes (23), and cellular defence mechanisms against oxidative stress (24). Advancements in systems biology and molecular level multi-omics analysis, allow us to investigate the complex interactome between NRF2-related cellular signalling pathways and highlight its potential involvement in diseases from cancers (25) and cardiovascular disease (26), to neurodegeneration (20)(27). This has led to discussions regarding the benefits of NRF2 as a therapeutic target (21,28). Furthermore, a more complete understanding of NRF2's activity and signalling interactome may inform on future personalised medicines (29,30). As a transcription factor, NRF2 activates the expression of various genes involved in protecting cells from damage caused by reactive oxygen species (ROS) (31), heavy metals (32), and other environmental stressors (33). Under normal 'healthy' conditions, NRF2 is sequestered in the cytoplasm through association with the Kelch-like ECH-associated protein 1 (Keap1) dimer, which facilitates ubiquitination and degradation of NRF2 via the Cullin 3-RING-box protein 1 complex (CUL3-RBX1) (33,34) (Figure 1a, top). However, under oxidative stress, ROS disrupt NRF2-Keap1 interactions, permitting the translocation of NRF2 into the nucleus (Figure 1a, bottom). Here NRF2 heterodimerises with small Maf (sMaf) proteins and binds to antioxidant response elements (AREs) within promoter regions of its specific gene targets, initiating the transcription of antioxidant and cytoprotective genes to counteract ROS (35,36) (Figure 1a, bottom).

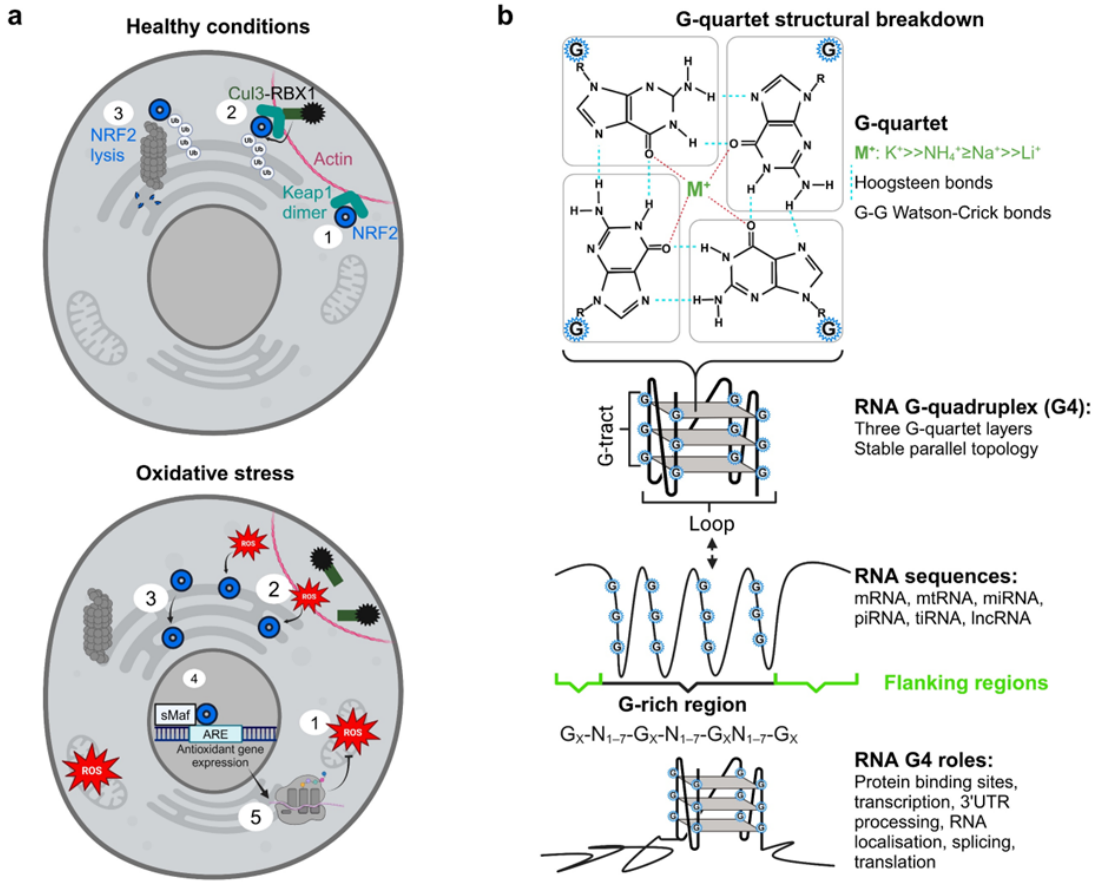

Figure 1. Schematic representation of a) the NRF2 signalling pathway in basal and oxidative stress response and b) the layered structure of RNA G-quadruplexes and general functions.

The activity of NRF2 is not only regulated by signalling pathways (37) but also by the structural features of its mRNA (38). The most canonical structure of RNA molecules are double helices which are formed by Watson-Crick hydrogen bond patterns between base pairs. Alternative Hoogsteen hydrogen bond base pairings form in non-Watson-Crick patterns to form increasingly structured helixes such as triplexes and quadruplexes (39). The 5′ UTR of NRF2 mRNA, contains guanine-rich sequences that can form secondary RNA tetra-helical structures called G-quadruplexes (G4s) (40) (41)

 doi:10.20944/preprints202601.1129.v1

(Figure 1b). The first step in forming a G4 is a G-quartet. This is formed by 4 guanine bases interacting via a combination of Hoogsteen and Watson-Crick hydrogen bonds, stabilised by a central monovalent cation (M^+) (Figure 1b, top). The cation that forms the strongest interaction within the G-quartet is potassium (K^+), although other cations may also be centralised such as ammonium ($NH4^+$), sodium (Na^+), and lithium (Li^+) which have increasingly weaker interactions (Figure 1b, right top) green text (42). Three stacked G-quartet layers with stable parallel topology, linked to loop regions, form the ultimate RNA G4 quadruplex structure (Figure 1b, middle). G4 forming G-rich regions found in many mRNAs, are characterised flanked by loop sequences (Figure 1b, bottom). G4s in other mRNA's have been found to have many effects including an influence on translation through stability adjustment (43), accessibility for ribosome binding (44), and the efficiency of translation initiation (45). Here, results indicate the potential presence of such a G4 in the 5'UTR of NRF2's mRNA and potential methods for investigating its function during different cellular conditions, and therapeutic avenues are discussed.

The structural integrity of both the mRNA and the associated regulatory proteins plays a pivotal role in NRF2 activation (46). Changes in the RNA's secondary structure (47), or in the interactions between RNA-binding proteins and the mRNA (48), can have profound effects on NRF2's ability to respond to stress (49), affecting not only its activation but also its ability to regulate genes that control cellular defence mechanisms (50). NRF2's role as a master regulator of several interacting cellular signalling pathways places it in a key position to be dynamically regulated by G4s which have been shown to be modulated under different cellular conditions, such as cellular stress (51). Such a mechanism would allow for controlled responses to environmental cues. Disruptions in the formation of NRF2's structural elements have been shown to contribute to several diseases (25)(20). Thus, a more thorough understanding of how the structural formations in NRF2 mRNAs influence its regulatory role may open new possibilities for targeted therapeutic interventions.

To investigate the presence of a G4 in the 5′ UTR of NRF2's mRNA, a series of computational and experimental techniques were employed (52). Initially, a series of bioinformatics tools were used to predict whether these structural motifs exist within the NRF2 RNA sequence (53–56). To validate in silico predictions, we designed minigenes corresponding to the NRF2 mRNA's 5′ UTR to assess the potential for G4 structural formations. We utilized an electrophoretic mobility shift assay (EMSA) (57), with a commonly used G4-specific antibody called 1H6 IgG (58) to investigate G4 formation. The EMSA is a fundamental technique involving the use of polyacrylamide gel electrophoresis (PAGE) to determine protein-nucleic acid interactions(59). Protein-nucleic acid complexes are larger than separate molecules so diffuse more slowly through the gel, hence if our minigenes interacted with the 1H6 antibody, they migrated less distance than unbound RNA. Next, we aimed to manipulate this interaction using pyridostatin (PDS) (60,61), a small molecule known to stabilize G4 structures (62). The effect of PDS binding to the NRF2 5′ UTR was assessed by fluorescence emission spectroscopy (63). By quantifying the association of 1-50 μM of PDS with 1 μM of RNA, the disassociation constant (K_d) was calculated (64). The dissociation suggests how strongly two molecules interact and is given as a concentration (μM) at which a half the complex will separate into individual component molecules. Although, this K_d does not always directly relate to in vivo binding efficiency since local concentration, ligand accumulation, and cooperative effects can also enhance in-cell associations. Here, the K_d was measured by plotting the fractions of RNA-complexed vs individual proteins and performing non-linear regression (65). The overall goal was to directly measure the formation and stabilization of RNA G4s in NRF2's 5′ UTR and assess their potential functional relevance.

2. Materials and Methods

2.1. In Vitro Transcription and Purification of NRF2 5′ UTR RNA

Three complementary bioinformatic structural analysis tools: RNAfold (66), QGRS Mapper (55), and G4Hunter (56), were used to assess the human NRF2 gene's (Ensembl ID: ENSG00000116044)

 doi:10.20944/preprints202601.1129.v1

5′UTR (NCBI RefSeq accession number: NM_006164.4) and investigate the presence of a G4 structure. The predicted G4 forming section (spanning nucleotides -197 to -158) was synthesized as two complementary DNA oligonucleotide sequences 5′-GTGGGGCGGGAGGCGGAGCGGGGCAGGGGCCC GCCGGCG-3′and 5′-CACCCCGCCCTCCGCCTCGCCCCGTCCCCGGGCGGCCGC-3′ (**Online Resource 1a**). The two sequences were annealed in a 1: 1 molar ratio to form the DNA template for PCR (67). This PCR amplification was performed to generate the transcription template (minigene) for in vitro RNA synthesis and was performed using primers designed to incorporate the T7 RNA polymerase promoter sequence. This is a common molecular technique adapted from (68). The forward primer (5′-TAATACGTGGGGCGG-3′) contains the T7 promoter (TAATAC) sequence, and the reverse primer (5′-GCGGCCGCCCGGGGA-3′) is complementary to the end of the NRF2 5′ UTR G-rich region (**Online Resource 1b**).

The transcription reaction was prepared to a 50 µL final volume including: 40 mM Tris-HCl pH 7.5, 20 mM $MgCl_2$, 10 mM NaCl, 2 mM spermidine HCl, 10 mM DTT, 4 mM rNTPs, 5% RNaseOUT (Invitrogen), 10 ng/µL PCR template, 5% T7 polymerase (1: 20 dilutions, homemade). The reaction was placed at room temperature for 10 minutes to allow for proper mixing, followed by incubation for 4 hours at 37 °C for transcription. After the transcription reaction, 1 unit of DNase I (Promega) was added for 30 extra minutes at 37 °C to degrade any remaining DNA template. Termination was achieved through a 10-minute 65 °C incubation. RNA was purified using an S-300 spin column (GE Healthcare), followed by a standard phenol-chloroform extraction to remove residual contaminants. RNA was precipitated at -20 °C for 30 minutes with 2.5 volumes of ethanol. Centrifugation created an RNA pellet which was collected, washed with 70% ethanol, and air-dried. The purified RNA was resuspended in RNase-free water and frozen in -80 °C. RNA concentration was assessed using a spectrophotometer by measuring absorbance at 260 nm. RNA fragments were determined pure with an A260:A280 ratio of approximately 2.0 according to the Thermo scientific Nanodrop spectrophotometer technical bulletin T042. Finaly, the integrity of the RNA was confirmed by electrophoresis at room temperature on a 1% agarose gel, ensuring the absence of degradation products (**Online Resource 2a**).

2.2. 5′ End Labelling of RNA Oligonucleotides

RNA oligonucleotides were 5′ end-labelled using a standard procedure with T4 polynucleotide kinase (PNK) (New England Biolabs) and [γ-32P] ATP (Perkin Elmer) (69). The labelling reaction was set up by combining the following components in a final volume of 20 µL at room temperature: 1× PNK reaction buffer (New England Biolabs), 2.5 µM RNA oligonucleotide template, 0.33 µM [γ-32P] ATP (specific activity: 3,000 Ci/mmol, 10 mCi/mL; Perkin Elmer), 10 U of T4 polynucleotide kinase (PNK) (New England Biolabs). The reaction was placed at 37 °C for 1 hour to allow for phosphorylation of the RNA 5′ end. Following incubation, the labelled RNA was separated by electrophoresis on a 15% denaturing polyacrylamide gel (6 M urea, 1× TBE buffer (89 mM Tris base, 89 mM boric acid, 2 mM EDTA), and 15% acrylamide (19: 1 bisacrylamide) solution (Accugel)) for 3 hours at 18 Watts. After electrophoresis, the band corresponding to the labelled RNA was excised from the gel. The RNA was then purified by ethanol precipitation. The gel slice was incubated with 300 mM sodium acetate and centrifuged at 13,000 rpm for 15 minutes. The resulting pellet was washed with 200 µL of pure ethanol and dried under vacuum for 30 minutes. After purification, labelled RNA was resuspended in RNase-free water for subsequent experiments.

2.3. Electrophoretic Mobility Shift Assay

EMSA was adapted from experiments described in past papers (57). Here, DNase I-treated 5′ end-labelled NRF2 5′ UTR mRNA was denatured by incubating at 95 °C for 5 minutes, then slowly cooled to room temperature overnight. The pure RNA was then incubated with the 1H6 antibody at 0, 1, 5, 10 µM concentrations. The RNA and antibody mixture was incubated at 30 °C for 10 minutes in a microtiter plate to allow for complex formation. For gel preparation, the RNA-antibody mixture

 doi:10.20944/preprints202601.1129.v1

was combined 1: 1 with native bromophenol blue and xylene cyanol gel dyes with 50 mM Tris and 50 mM Glycine. The samples were then added onto a 2.5% (w/v) native Low Melting Point (LMP) agarose (Invitrogen) gel in 1× Tris/Glycine buffer (50 mM Tris, 50 mM Glycine). Electrophoresis was performed at 4 °C at 80 V for 2.5 hours in 1× Tris-Glycine buffer. Following electrophoresis, the gels were compressed and dried overnight under vacuum. After drying, the gels were scanned using a Typhoon scanner with a phosphor imaging screen to visualize the labelled RNA. The scanned images were analysed and quantified using OptiQuant software to determine the size of RNA-antibody complexes and the relative binding efficiency at varying antibody concentrations.

2.4. Fluorescence Assays

Fluorescence assays and concentrations of reagents chosen were adapted from a previously described technique (63). In our experiment the mRNA fragment in-vitro transcribed in section 2.1 (GTGGGGCGGGAGGCGGAGCGGGGCAGGGGCCCGCCGGCG), was prepared at a final concentration of 1 μM. This ensured reliable fluorescence detection and binding signal while maintaining physiological relevance and avoiding RNA aggregation. The PDS (MERCK SML2690) was added to 1, 2, 5, 10 and 50 μM, to span a full titration range for fluorescence binding assays, allowing accurate determination of binding affinity. The RNA-PDS mixture was prepared in G4-forming buffer (10 mM KCl, 10 mM Tris-HCl pH 7.5 and 1 mM $MgCl_2$). The solution containing the 1 μM NRF2 mRNA and specific concentrations of PDS was carefully mixed in a Hellma fluorescence cuvette (Suprasil® quartz cuvette, with a spectral range of 200-2500 nm and a path length of 10 × 2 mm, chamber volume of 100 μL). The cuvette material and specifications (Suprasil®) were chosen to minimize background fluorescence and allow optimal signal detection for RNA fluorescence assays. The fluorescence emission was recorded at room temperature by using FluoroMax-4. The excitation wavelength was set to 555 nm, which is optimal for the excitation of PDS-bound RNA (70). Emission spectra were collected from 350 nm to 700 nm, as this range encompasses the characteristic emission maxima observed for PDS-bound G-quadruplexes. Previous studies showed that PDS exhibits enhanced fluorescence upon G4 binding, with emission maxima typically observed around **610–620 nm** (70). The spectra were recorded in 1 nm intervals to ensure accurate resolution of emission features, with the data being collected in scan mode for a full emission profile.

3. Results

To investigate the potential for G4 formation in the 5′ UTR of NRF2 RNA under basal conditions, we employed three bioinformatics tools: RNAfold (66), QGRS Mapper (55), and G4Hunter (56). The sequence of the NRF2 5′ UTR analysed was the same as amplified for in vitro transcription as described in section 2.1: 5′-GTGGGGCGGGAGGCGGAGCGGGGCAGGGGCCCGCCGGCG-3′. We compared the predictions from these tools to assess their ability to identify G4 forming regions within this RNA segment (**Online Resource 3a-c**). RNAfold was applied to predict G4 forming regions based on folding energy and sequence motifs. It suggested that the 5′ UTR sequence 5′-GTGGGGCGGGAGGCGGAGCGGGGCAGGGGCCCGCCGGCG-3′ is likely to harbour a highly stable G-quadruplex structure. The tool highlighted the segment 5′-GTGGGGCGGGAGGCGGAGC-3′, which forms a G4 structure of three G-tracts (5G, 3G, 3G) separated by **1-nucleotide loops** (C and A), forming a predicted **3-tetrad G4** with short loop lengths typically associated with **highly stable G4 structures.** RNAfold predicted minimum free energy (ΔG) of -6.9 kcal/mol supporting the idea of a strongly structured G4. This region includes a highly conserved G-rich motif 5′-GGGGGCGGGAGGG-3′, in agreement with previously identified G4 forming sequences. The predictions from QGRS, and G4Hunter were also consistent in identifying a G4-forming region of the NRF2 5′ UTR 5′-GTGGGGCGGGAGGCGGAGC-3′. All three tools highlighted the same G-rich sequence 5′-GGGGGCGGGAGGG-3′, supporting the likelihood of G4 formation. These results indicate that the formation of G-quadruplex structures in this region is likely which could potentially play a regulatory role in NRF2 expression, either by influencing RNA stability or translation efficiency. To further investigate the potential significance of the proposed rG4 complex in NRF2's

 doi:10.20944/preprints202601.1129.v1

5′UTR, we aligned several representative mammalian NRF2 5′ UTR sequences to explore evolutionary conservation. Despite 5′ UTR sequences being typically less conserved across species than coding regions, the G-rich tract highlighted by the three predictive software's is partially conserved, likely in a manner that would preserve G4 structural formation (supplementary figure).

To experimentally verify the G-quadruplex formation and assess the binding of the 1H6 antibody to the NRF2 5′ UTR, we conducted EMSA using varying concentrations of the 1H6 antibody (Figure 2). The experiment was run on a LMP gel to assess the binding of the G4 structure without denaturing the RNA. The NRF2 5′ UTR RNA fragment 5′-GTGGGGCGGGAGGCGGAGCGGGGCAGGGGCCCGCCGGCG-3′ was incubated with increasing concentrations of the 1H6 antibody (ranging from 1 to 10 μM) in a binding buffer optimized for G4 stabilisation (Figure 2a, left). As the concentration of the 1H6 antibody increased, we observed a clear shift in the mobility of the RNA on the native gel. At higher antibody concentrations (1 μM and above), a distinct slow migrating band appeared, which is consistent with the formation of a stable RNA-1H6 antibody complex. In negative control experiments, we used a no antibody, which did not result in any detectable mobility shift, confirming the specificity of the interaction between the 1H6 antibody and the G4 structure (Online Resource 2b). The 1H6 antibodies efficiency to an alternative positive control G4 was not included here but has been shown in previous publications (71). Furthermore, we used a G4-disrupting mutant where six G residues in the within the G4 core sequence **5′-GGGGGCGGGAGGG-3′,** were substituted with adenines (A) (positions 3–6 and 10–11) resulting in the G4 disrupting mutant sequence: (5′-GTAAAACGGGAGACGGAGCGGGGCAGGGGCCCGCCGGCG-3′). This modified sequence prevents G-tetrad stacking required for G-quadruplex formation. With this mutant we saw significantly reduced mobility shift with a of the NRF2 5′ UTR, further confirming that the observed shift was dependent on the presence of a stable G4 structure in the RNA.

 doi:10.20944/preprints202601.1129.v1

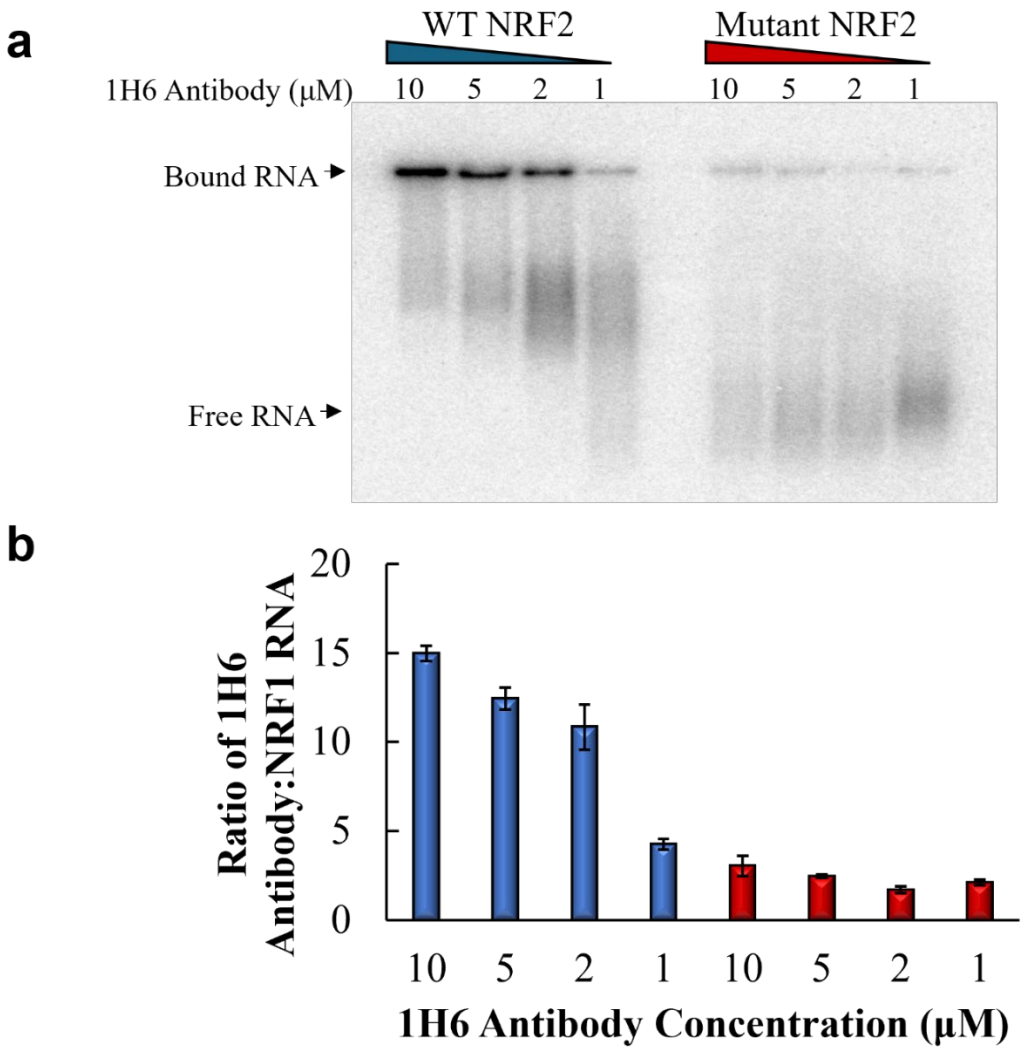

Figure 2. EMSA gel picture and ImageJ quantification of NRF2 RNA G-quadruplex binding to 1H6 antibody at various concentrations, error bars show standard deviation between biological replicates (*n*=2).

The 2.5% LMP agarose gel picture shows both WT (**left**) and mutated NRF2 5′ UTR (**right**) RNA G4s binding to 1H6 AB in a variety of concentrations (1, 2, 5, and 10 μM). In the WT condition free RNA shifts upwards due to binding to 1H6 AB as the formation of RNA G4s occur. The mutated form (Gs to As) does not show the same upward shift as the RNA G4s do not form anymore (Figure 2a). The bar graph shows the ratio of band intensities of each lane both in WT and mutated condition normalised to no 1H6 AB condition in each concentration measured by ImageJ tool (Figure 2b, Online Resource 4).

To further characterize the G-quadruplex structure formed by the NRF2 5′ UTR RNA, we performed a fluorescence spectroscopy including pyridostatin which selectively binds to RNA G-quadruplexes, resulting in a change in fluorescence emission due to the interaction with the G4 structure (Figure 3). This assay allowed for the determination of binding affinity based on fluorescence intensity across wavelengths (Online Resource 5) and provided insight into the formation and stabilization of G-quadruplexes in the NRF2 5′ UTR RNA. Following incubation, the fluorescence emission spectra of the DNA-free pyridostatin-RNA complexes were measured between 500–600 nm which represents the emission range of pyridostatin when bound to RNA G4 structures (Figure 3). A sharp increase in fluorescence intensity at approximately 555 nm was expected as pyridostatin binds to the G4 structure, and any shift or change in intensity would indicate stabilization of the G4 conformation by pyridostatin (Figure 3a). A control sample containing only RNA and no pyridostatin was included to measure the baseline fluorescence. The fluorescence

 doi:10.20944/preprints202601.1129.v1

spectroscopy binding assay confirmed the creation of a stable G-quadruplex structure in NRF2's 5′ UTR and demonstrated that pyridostatin binds specifically to the G4 structure. The fluorescence emission spectra showed a clear, concentration-dependent increase in intensity upon pyridostatin binding. The dissociation constant (K_d) for binding of PDS to NRF2 RNA is calculated by linear regression using Python and MATLAB tools (Online Resource 6a-b). The K_d value of 29.82 μM indicates a relatively strong interaction between pyridostatin and the NRF2 RNA G-quadruplex (Figure 3b), which agrees with previous RNA G4 measurements from Hou et al., 2022.

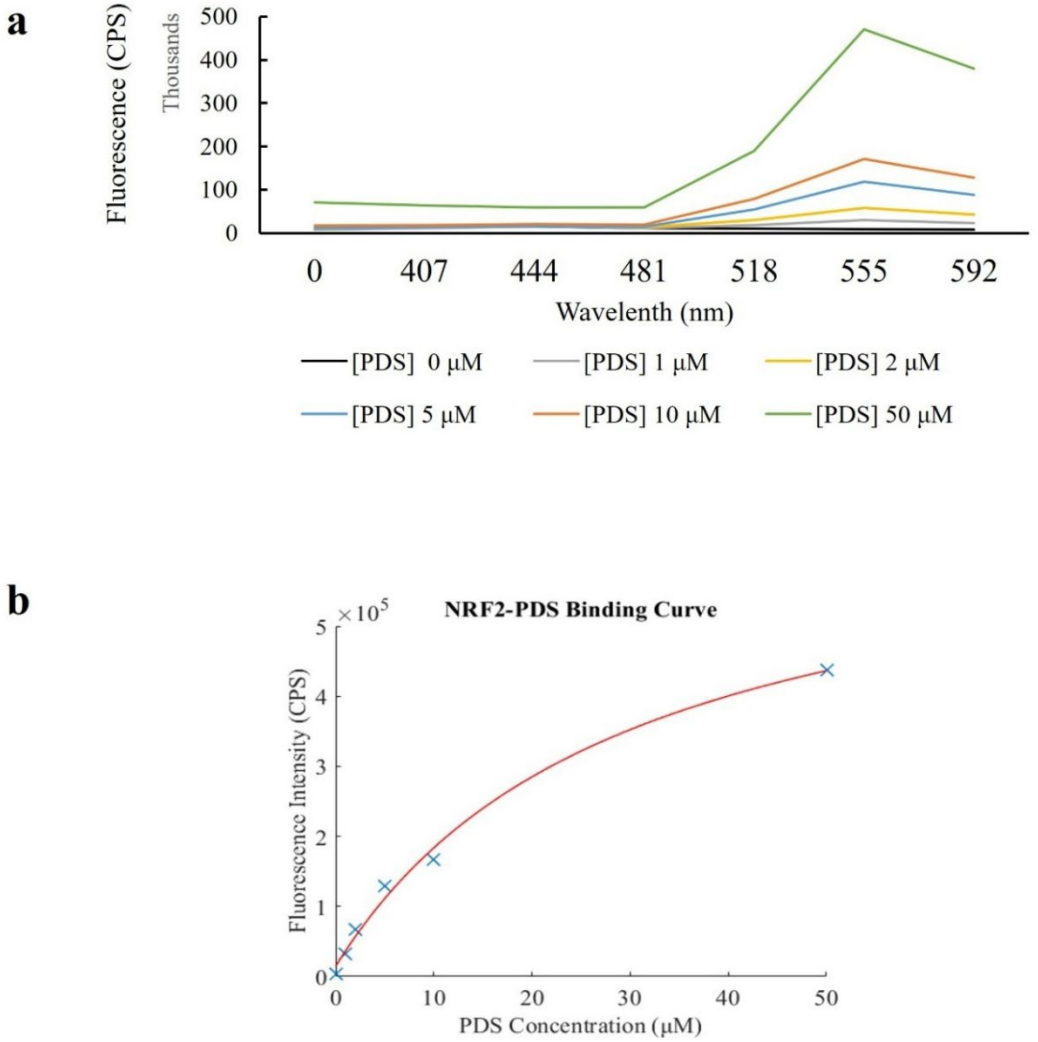

Figure 3. Line graph and a binding curve showing the interaction of PDS with 5′ UTR G4 forming NRF2 RNA sequences at different concentrations of pyridostatin (PDS).

Fluorescence emission spectra of free PDS (dark blue) and 1 μM (grey), 2 μM (yellow), 5 μM (light blue), 10 μM (orange) and 50 μM (green) PDS in the presence of NRF2 RNA. RNA was incubated at a concentration of 1 μM with PDS at increasing concentrations at excitation wavelength 380 nm.

These findings further support the possibility of a functional G-quadruplex in NRF2's 5′ UTR and suggest that pyridostatin could be used as a tool for modulating G4 structures in RNA, which we hypothesise may influence post-transcriptional regulation of NRF2 expression.

4. Discussion

This study aimed to elucidate a potential formation of G4 structures in NRF2 RNA's 5′ UTR region and their implications in regulating NRF2 expression. Using three bioinformatics tools:

 doi:10.20944/preprints202601.1129.v1

RNAfold, QGRS, and G4Hunter, we consistently identified a G4-forming region within the NRF2 5′ UTR. All three tools highlighted the G-rich sequence GGGGGCGGGAGGG as a likely candidate for G4 formation (**Online Resource 3a-c, 7**). The high consistency across the predictive tools reinforces the reliability of these findings, particularly the prediction by RNAfold which showed this G4 structure is highly stable, with a folding energy of -6.9 kcal/mol. To extend our bioinformatic investigation, we aligned a few representative mammalian NRF2 5′ UTR sequences which indicate there may be some evolutionary conservation of this sequence (**supplementary resource**). Next, to support the in silico analysis, EMSA and fluorescence spectroscopy techniques were applied. The EMSA experiments, quantified with Image J software, provided experimental evidence supporting the bioinformatics predictions. The mobility shift observed with increasing concentrations of the 1H6 antibody confirmed the formation of a G4 structure in the NRF2 5′ UTR RNA. Importantly, the absence of a shift in G4 mutant negative controls validates the necessity of this sequence for antibody interaction and thus G4 formation.

These in vitro results suggest that the predicted G-quadruplex is indeed formed under the experimental conditions and may have functional relevance. We further validated the bioinformatics and EMSA with the fluorescence spectroscopy assay to further characterise the G4 structure by its association with a G4 binding molecule called pyridostatin (62). The observed concentration-dependent increase in fluorescence intensity again supported the predicted presence of a G4 structure within this section of the NRF2 5′UTR, due to an interaction between pyridostatin and the G4 structure. The calculated dissociation constant (K_d) of 29.82 μM indicates a solid binding affinity for an RNA G4. Other RNA G4's has been discovered with similar micromolar affinities (72)which indicates that, depending on cellular context, this interaction should be physiologically viable in vivo. Further experimental validation, such as G4-specific RNA probes or structural assays, could be applied to confirm these predictions and elucidate their functional significance. Regarding PDS, its association with known DNA G4s in vitro is typically even stronger than our determined NRF2 RNA-G4 value. Hence it was essential for the RNA in this paper's EMSA's to be DNA-free. For example, one paper found PDS bound to G rich DNA strands TERRA and Telomere repeat DNA (TeloDNA) known to form DNA G4 structures with K_ds of 0.66 μM and 0.05 μM respectively(73). PDS was also identified as a non-sequence-selective ligand for G4s which associated with the NRAS DNA G-quadruplex with a K_d of 4.1 ± 0.1 μM (74), and binding Zika virus RNA G-quadruplexes in vitro with a K_d of 4.2 ± 0.4 μM. Although these values show higher affinity binding of PDS to G4s is possible, these are DNA G4's, suggesting PDS may have a higher affinity for DNA G4's than RNA G4's. Therefore, we also compared our affinity with other RNA G4 targeting molecules in initial drug screens. For example, a molecule termed 'F1' bound to a G4 in human DHX15's 5′UTR with a K_d of 12.6 μM (75), and 'oxymatrine' which provided a K_d of 37.5 μM associating with a G4 in human vascular endothelial growth factor (hVEGF) mRNA (75). These findings highlight that PDS association with our NRF2 G4 is strong enough to be considered for initial in vivo analysis, and highlights that in the future, therapeutic ligands with even stronger affinity for NRF2 G4 could be designed.

Other RNA G4s function to influence mRNA splicing and modulate isoform production, affect biogenesis of ncRNAs and their functions (76,77), effect transport of the mRNA depending on protein co-factor association, and effect translation (78–81). G4s have already been linked to oxidative stress which may also point a link to the G4 in NRF2 's 5′UTR that we investigated here (82,83). Specifically, when in the 5′UTRs of some mRNAs, G4s have been revealed as potential therapeutic targets, such as the G4 in cyclin D3 mRNA which helps regulate the cell cycle and whose disruption has been implicated in cancers (84). Therefore, it would be intriguing to also follow up the G4 we identify in NRF2's 5′ UTR for therapeutic intervention. However, many optimisations would be required before use.

While our EMSA and fluorescence spectroscopy are robust methods, they do not provide all the answers which are essential before therapeutic investment (85). The first step may be to confirm the exact structure of our proposed rG4 including parallel/antiparallel orientation and tetrad number**.** To

 doi:10.20944/preprints202601.1129.v1

elaborate on these structural dynamics, CD spectroscopy may be the logical next step, followed by higher-resolution NMR as resources allow. It is also important to consider that alternative structures such as hairpins may coexist with the G4 in the NRF2 5′ UTR therefore SHAPE-MaP could be employed as it is the gold-standard method to probe structural heterogeneity in cells. Next, the functional in vivo significance of this suggested NRF2 G4 should be explored including its possible effects on the cells oxidative stress response. Currently, NRF2's G4-related response to oxidative stress remains speculative. Modulation of NRF2's 5′ UTR G4 stability likely plays a critical role in fine-tuning NRF2 translation, thereby influencing the timing and magnitude of cellular antioxidant responses. However, there are several possibilities for exactly how this occurs. Under basal conditions, stable G4 structures may act as translational repressors limiting NRF2 protein synthesis to maintain homeostasis and prevent unwarranted activation of the antioxidant pathway (86,87). Upon oxidative or electrophilic stress, dynamic remodelling or destabilization of these G4 motifs potentially mediated by helicases or RNA-binding proteins could rapidly relieve translational repression, facilitating a timely increase in NRF2 levels. In this case, pharmacological stabilization of the G4 with ligands like pyridostatin may prolong the repressive state, attenuating NRF2 translation and downstream antioxidant gene expression to reduce NRF2 overactivity in diseases such as certain cancers where NRF2 confers chemoresistance (20). Conversely, G4 formation in NRF2's 5′UTR may increase translation most commonly by stimulating cap-dependent translation initiation by recruitment of the 40S small ribosomal subunit via eukaryotic initiation factors (eIFs) (88,89). This is relatively common for RNA G4s (90), and has been suggested in a previous paper where the removal of the 5′UTR resulted in an unresponsive NRF2 mRNA which was not induced by H2O2 during oxidative stress (91). They found that loss of a 5′UTR G4 complex prevented elongation factor 1 alpha (EF1a) from associating with NRF2 mRNA transcript, thereby reducing translation. Therefore, if NRF2 expression is no longer enhanced upon oxidative stress, then it cannot upregulate the expression of antioxidant genes as per its normal function. Dysregulation of NRF2 in such a way is linked to various diseases including cardiovascular (92), Huntington's (27), cancers and more generally across neurodegeneration (20). Hence it has great value as a therapeutic target.

Although current results suggest a regulatory role, direct evidence linking the G4 structure to NRF2 expression regulation or cellular responses is lacking, especially relating to the timing or magnitude of NRF2 activation in response to stress. Investigating how G4 stability influences the kinetics of NRF2 activation including the onset, peak, and duration of protein expression following stress is therefore crucial. Time-course experiments measuring NRF2 protein and target gene induction, coupled with real-time monitoring of G4 folding status (e.g., via live-cell RNA imaging, chemical shift mapping NMR spectroscopy or Forster Resonance Energy Transfer), would provide valuable mechanistic insights into this regulatory layer (93,94). Other functional studies such as luciferase reporter assays, RNA-binding protein knockdowns/overexpression, or CRISPR-CAS9 experiments are required to establish if NRF2 expression is changing upon G4 binding in vivo. Luciferase reporter assays have been applied in this manner before to investigate c-MYC transactivation in NM23-H2 binding to a DNA G4 motif within the cMYC gene (95). For NRF2, reporter constructs containing the wild-type versus G4-disrupting mutant NRF2 5′ UTR sequences could be transfected into cells to quantitatively assess the impact of G4 formation on translational efficiency and RNA stability in living cells. Luciferase reporter assays are useful as they are quick and provide precise quantitative results but have limitations too. The main limitation is that the levels of mRNA produced from the plasmid is difficult to reflect endogenous levels, so they do not completely reflect in vivo conditions which may be an issue if binding efficiency depends on concentration(96). Alternatively, CRISPR-Cas9 could be used to create an endogenous NRF2 mutant that can no longer form the G4 and investigate the effect on the cell's response to oxidative stress with phenotypic cell culturing experiments (97). The disadvantage here is that strain generation takes longer, but apart from the mutation, endogenous transcription and translation are maintained meaning optimal investigation of the cellular effect of G4 removal is possible. Finaly, CRISPR or siRNA interference techniques could be used to knockdown RNA binding proteins known to interact with G4's such as

 doi:10.20944/preprints202601.1129.v1

helicases (98), to evaluate their roles in modulating NRF2 G4 structure stability, consequent NRF2 expression changes, and oxidative stress response. Although this will be more useful once a clear target to investigate is discovered as cause-and effect of NRF2's G4 and the knocked down protein will not be clear.

Once the role of NRF2's G4 in response to oxidative stress is elucidated in vivo, therapeutic drug design may be established. Firstly, screening methods are required to find compounds that associate with sufficient efficiency and selectivity. This can be completed in silico via computational docking which predicts ligands for structure-based drug discovery, so is commonly used for G4-targeted therapeutic development (99). There has been shown to be inconsistencies with the results from various docking software's such as AutoDock Vina, DOCK6, Glide, and RxDock, which was investigated in a paper looking to design a drug targeting a G4 in the MYC promotor (100). They concluded that current in silico docking platforms are relatively unreliable and should be used with care. Therefore, biochemical and biophysical high-throughput screening techniques can be employed in tandem within silico approaches (101). For example, small molecule microarrays have been employed recently alongside in silico analysis to discover BMVC, a drug that can target the aforementioned G4 in the MYC promotor (102).

Structure-based in silico and biochemical drug screens would benefit from complementary in-depth structural analysis like Nuclear Magnetic Resonance (NMR) spectroscopy or x-ray crystallography which could offer more definitive insights into the G4 structure to get a clear prediction of potential therapeutic molecules (102,103). X-ray crystallography requires careful trial-and-error adjustment of several aspects of the buffer including pH, temperature, ion concentration and precipitant size/concentration, to optimize crystal formation (104), however imaging is much more straightforward once the crystallised structure. In the case of large protein-RNA complexes crystallisation may be impossible. NMR measure's structure determined by the spinning of protons in hydrogen atom nuclei, it is more difficult to perfect than x-ray crystallography but more useful for imaging dynamics over time with chemical shift mapping (93). NMR can also struggle to determine large complexes, although isotope and segmental labelling techniques have been applied in the past to investigate complicated structures such as ribonucleoprotein complexes (105). In the case of visualising large, complicated structures, cryo-electron microscopy (Cryo-EM) could be employed which involves electron microscopy at cryogenic temperatures to detect the electron density and generate a map of protein-RNA structure. However, the resolution of the image generated is lower than X-ray crystallography, so the fine points of G4 structure may remain elusive. Finaly, single-molecule tools like Forster Resonance Energy Transfer (smFRET) have previously been applied to investigate G4s (94,106,107). Similarly to NMR, smFRET can visualize dynamics and interactions between short RNA sequences (~50-100 nts) labelled RNA and proteins (108). However the fluorophore labels can affect RNA folding and function, so the location of fluorophores on the DNA construct needs to be tightly controlled and the ionic conditions of the experiment need to be highly regulated to allow simultaneous G4 formation and fluorescence imaging. Despite these difficulties, the kinetic and mechanistic data from FRET can synergize well with static structural data from x-ray crystallography or Cyro-EM. Overall, each high-resolution imaging method has pros and cons and best would be to apply these techniques in tandem to enable more detailed structural analysis of NRF2 Gf complex formation (109). Together in silico and biochemical screening within high resolution imaging approaches can be applied to the G4 in NRF2 to discover potential therapeutic ligands.

After screening, several rounds of structural optimisations of ligands may be required before a ligand of adequate strength, minimal off target effects, and minimal toxicity can be designed (110). Effective delivery of small molecules like PDS to target tissues and sub-cellular compartments remains a significant hurdle. Strategies such as nanoparticle-based delivery systems (111) or conjugation to targeting moieties (112)already implemented in gene therapies, may be necessary to enhance bioavailability and tissue specificity. Another optimisation required would be to design the drug to limit off-target effects. Off target effects represent a major concern due to the high prevalence

 doi:10.20944/preprints202601.1129.v1

of G-quadruplex motifs throughout the transcriptome (total mRNAs) and translatome (mRNAs being actively translated by ribosomes). Small molecules that are designed to bind specific G4 structures may also inadvertently stabilize or disrupt other RNA or DNA G-quadruplexes, leading to unintended gene regulation changes or toxicity. Antibodies already exist that can preferentially target RNA G-quadruplexes over DNA G quadruplexes (113) but for more specific targeting, structure-based drug design and rigorous selectivity screening will be essential to minimize these risks (114)

Finally, RNA G4 dynamics are often influenced by cellular context and interacting proteins, suggesting that context-dependent cellular variability could affect therapeutic efficacy. Cellular factors that could influence G4 formation and stability include RNA-binding proteins (RBPs), secondary RNA structures, and intracellular ionic conditions. It is well known that G4 complexes are targets for RBPs which are often required for the physiological effect of the RNA G4 (81). In vivo it has also been suggested cytosine methylation may influence RNA G quadruplex formation. It is possible other RNA modifications such as m7G methylation also effect RNA G-quadruplex structures, possibly acting as rapid switches to activate or inactivate the G-quadruplex folding (115). This could be one mechanism for how NRF2's G4 contributes to oxidative stress response, if the G rich element is methylated to trigger formation of the G quadruplex and initiate its transcription factor activity. Finaly, in vitro, G4 structures are induced by cationic concentrations, most often K^+ (116), so it is possible influx of K^+ in vivo may also act as an initiator of G4 folding and be used to initiate the translation of NRF2 to boost antioxidant genes transcription upon oxidative stress. Each of these effects would be missed or exaggerated in our bioinformatics and in vitro experiments, highlighting the need for comprehensive in vivo experiments as the next stage of testing NRF2 G4 cellular function to evaluate pharmacodynamics, toxicity, and long-term effects. There are options for in vivo profiling of the NRF2 3′ G4 in vivo with G4 specific probes. For example, fluorescent ligands like pyridostatin, BRACO-19, TMPyP4, and Ber can be applied to cells (117–119). These cells can be tested for fluorescence with flow cytometry and immunofluorescence assays to investigate interactions. However, their analysis is limited by the same factors as NRF2 G4 therapeutic molecule design, by difficulties targeting probes to a subcellular location and a specific RNA-G4 of interest. There is also some difficulty visualizing fluorescence in certain subcellular localisations so new methods and ligands are being explored, such as the G4-ligand guided immunofluorescence staining approach with BrdU immune tag modified G4-ligands for vivo applications (107). For initial experiments pyridostatin could be used as a starting point for NRF2's G4 as we have shown a relatively strong interaction in vitro.

Despite the challenges discussed, there are many G4s already being exploited by design of small molecules or aptamers that can bind the G4 and effect translation for therapeutic purposes (75). For example, RNA G4 targeted degradation complexes have been developed to specifically degrade RNAs with G4s in an effort to inhibit Fragile X mental retardation protein (FMRP) whose overexpression has been associated with metastasis and immune evasion in cancers (120). Outside genetic defects, G4s have also been targeted for antiviral therapies (121). For example, the d(GGGT)4) or T30175 aptamers form G4 dimers recognised by the Human Immunodeficiency Virus (HIV) integrase protein, which then competes with viral G4 quadruplexes. Viral G4s are important for replication and by preventing HIV integrase binding, infectivity is inhibited (122,123). An alternative to aptamers is proteolysis-targeting chimeras (PROTACs) which degrade target proteins using the cells endogenous ubiquitin-proteasome system (124).This shows that although some major developments are required for G4 therapeutics, they are possible and could be applied to NRF2.

In conclusion, we have taken the first steps in identifying and validating an RNA G4 in the 5′UTR of NRF2 with a combination of bioinformatic and in vitro analysis. In vivo studies using G4-specific probes such as pyridostatin, in living cells could provide further insights into the relevance of this structure in cellular contexts. Additionally, structural studies employing high-resolution techniques could be applied to confirming the G4 topology and identify potential interactions with RNA-binding proteins or small molecules. These steps should reveal if NRF2's G4 is a therapeutic target for drug screening and disease treatments.

 doi:10.20944/preprints202601.1129.v1

Supplementary Materials: The following supporting information can be downloaded at the website of this paper posted on Preprints.org.

References

1. Boo SH, Kim YK. The emerging role of RNA modifications in the regulation of mRNA stability. Vol. 52, Experimental and Molecular Medicine. Springer Nature; 2020. p. 400–8.
2. Leppek K, Byeon GW, Kladwang W, Wayment-Steele HK, Kerr CH, Xu AF, et al. Combinatorial optimization of mRNA structure, stability, and translation for RNA-based therapeutics. Nat Commun. 2022 Dec 1;13(1).
3. Leppek K, Das R, Barna M. Functional 5′ UTR mRNA structures in eukaryotic translation regulation and how to find them. Vol. 19, Nature Reviews Molecular Cell Biology. Nature Publishing Group; 2018. p. 158–74.
4. Chang JW, Zhang W, Yeh HS, De Jong EP, Jun S, Kim KH, et al. MRNA 3′-UTR shortening is a molecular signature of mTORC1 activation. Nat Commun. 2015 Jun 15;6.
5. Narula A, Ellis J, Taliaferro JM, Rissland OS. Coding regions affect mRNA stability in human cells. 2019; Available from: http://www.rnajournal.org/cgi/doi/10.1261/rna.
6. Buxbaum AR, Haimovich G, Singer RH. In the right place at the right time: Visualizing and understanding mRNA localization. Vol. 16, Nature Reviews Molecular Cell Biology. Nature Publishing Group; 2015. p. 95–109.
7. Noller HF. Evolution of protein synthesis from an RNAworld. Cold Spring Harb Perspect Biol. 2012 Apr;4(4).
8. Cetnar DP, Hossain A, Vezeau GE, Salis HM. Predicting synthetic mRNA stability using massively parallel kinetic measurements, biophysical modeling, and machine learning. Nat Commun. 2024 Dec 1;15(1):9601.
9. Jia L, Mao Y, Ji Q, Dersh D, Yewdell JW, Qian SB. Decoding mRNA translatability and stability from 5′UTR [Internet]. 2020. Available from: http://biorxiv.org/lookup/doi/10.1101/2020.03.13.990887
10. Wei W, Gao W, Li Q, Liu Y, Chen H, Cui Y, et al. Comprehensive characterization of posttranscriptional impairment-related 3′-UTR mutations in 2413 whole genomes of cancer patients. NPJ Genom Med. 2022 Dec 1;7(1).
11. Chu Y, Yu D, Li Y, Huang K, Shen Y, Cong L, et al. A 5′ UTR Language Model for Decoding Untranslated Regions of mRNA and Function Predictions [Internet]. 2023. Available from: http://biorxiv.org/lookup/doi/10.1101/2023.10.11.561938
12. The role of the 5′ untranslated region of an mRNA in translation regulation during development.
13. Ryczek N, Łyś A, Makałowska I. The Functional Meaning of 5′UTR in Protein-Coding Genes. Vol. 24, International Journal of Molecular Sciences. MDPI; 2023.
14. Van Nostrand EL, Freese P, Pratt GA, Wang X, Wei X, Xiao R, et al. A large-scale binding and functional map of human RNA-binding proteins. Nature. 2020 Jul 30;583(7818):711–9.
15. Szostak E, Gebauer F. Translational control by 3′-UTR-binding proteins. Brief Funct Genomics. 2013 Jan;12(1):58–65.
16. Steri M, Idda ML, Whalen MB, Orrù V. Genetic variants in mRNA untranslated regions. Wiley Interdiscip Rev RNA. 2018 Jul 1;9(4).
17. Patel RK, West JD, Jiang Y, Fogarty EA, Grimson A. Robust partitioning of microRNA targets from downstream regulatory changes. Nucleic Acids Res. 2020 Sep 25;48(17):9724–46.
18. Kiltschewskij DJ, Harrison PF, Fitzsimmons C, Beilharz TH, Cairns MJ. Extension of mRNA poly(A) tails and 3′UTRs during neuronal differentiation exhibits variable association with post-transcriptional dynamics. Nucleic Acids Res. 2023 Aug 25;51(15):8181–98.
19. Strober BJ, Elorbany R, Rhodes K, Krishnan N, Tayeb K, Battle A, et al. Dynamic genetic regulation of gene expression during cellular differentiation HHS Public Access. Science (1979) [Internet]. 2019;364(6447):1287–90. Available from: https://doi.org/10.5281/zenodo.2590826.
20. Dinkova-Kostova AT, Kostov R V., Kazantsev AG. The role of Nrf2 signaling in counteracting neurodegenerative diseases. Vol. 285, FEBS Journal. Blackwell Publishing Ltd.; 2018. p. 3576–90.

 doi:10.20944/preprints202601.1129.v1

21. Papp D, Lenti K, Módos D, Fazekas D, Dúl Z, Türei D, et al. The NRF2-related interactome and regulome contain multifunctional proteins and fine-tuned autoregulatory loops. FEBS Lett. 2012 Jun 21;586(13):1795–802.
22. Nguyen T, Nioi P, Pickett CB. The Nrf2-antioxidant response element signaling pathway and its activation by oxidative stress. Vol. 284, Journal of Biological Chemistry. 2009. p. 13291–5.
23. Denicola GM, Karreth FA, Humpton TJ, Gopinathan A, Wei C, Frese K, et al. Oncogene-induced Nrf2 transcription promotes ROS detoxification and tumorigenesis. Nature. 2011 Jul 7;475(7354):106–10.
24. Bryan HK, Olayanju A, Goldring CE, Park BK. The Nrf2 cell defence pathway: Keap1-dependent and -independent mechanisms of regulation. Vol. 85, Biochemical Pharmacology. Elsevier Inc.; 2013. p. 705–17.
25. Jung BJ, Yoo HS, Shin S, Park YJ, Jeon SM. Dysregulation of NRF2 in cancer: From molecular mechanisms to therapeutic opportunities. Vol. 26, Biomolecules and Therapeutics. Korean Society of Applied Pharmacology; 2018. p. 57–68.
26. Dhyani N, Tian C, Gao L, Rudebush TL, Zucker IH. Nrf2-Keap1 in Cardiovascular Disease: Which Is the Cart and Which the Horse? Vol. 39, Physiology (Bethesda, Md.). 2024. p. 0.
27. Tucci P, Lattanzi R, Severini C, Saso L. Nrf2 Pathway in Huntington's Disease (HD): What Is Its Role? Vol. 23, International Journal of Molecular Sciences. MDPI; 2022.
28. Saha S, Buttari B, Profumo E, Tucci P, Saso L. A Perspective on Nrf2 Signaling Pathway for Neuroinflammation: A Potential Therapeutic Target in Alzheimer's and Parkinson's Diseases. Vol. 15, Frontiers in Cellular Neuroscience. Frontiers Media S.A.; 2022.
29. Wang RS, Maron BA, Loscalzo J. Multiomics Network Medicine Approaches to Precision Medicine and Therapeutics in Cardiovascular Diseases. Arterioscler Thromb Vasc Biol. 2023 Apr 1;43(4):493–503.
30. Jurisic V. Multiomic analysis of cytokines in immuno-oncology. Vol. 17, Expert Review of Proteomics. Taylor and Francis Ltd.; 2020. p. 663–74.
31. Ngo V, Duennwald ML. Nrf2 and Oxidative Stress: A General Overview of Mechanisms and Implications in Human Disease. Vol. 11, Antioxidants. MDPI; 2022.
32. Simmons SO, Fan CY, Yeoman K, Wakefield J, Ramabhadran R. NRF2 Oxidative Stress Induced by Heavy Metals is Cell Type Dependent [Internet]. Available from: http://www.ifti.org/cgi-
33. Kensler TW, Wakabayashi N, Biswal S. Cell survival responses to environmental stresses via the Keap1-Nrf2-ARE pathway. Vol. 47, Annual Review of Pharmacology and Toxicology. 2007. p. 89–116.
34. Heurtaux T, Bouvier DS, Benani A, Helgueta Romero S, Frauenknecht KBM, Mittelbronn M, et al. Normal and Pathological NRF2 Signalling in the Central Nervous System. Vol. 11, Antioxidants. MDPI; 2022.
35. He F, Ru X, Wen T. NRF2, a transcription factor for stress response and beyond. Vol. 21, International Journal of Molecular Sciences. MDPI AG; 2020. p. 1–23.
36. Glanzner WG, da Silva Sousa LR, Gutierrez K, de Macedo MP, Currin L, Perecin F, et al. NRF2 attenuation aggravates detrimental consequences of metabolic stress on cultured porcine parthenote embryos. Sci Rep. 2024 Dec 1;14(1).
37. Li R, Jia Z, Zhu H. Regulation of Nrf2 Signaling.
38. Kumari D, Gabrielian A, Wheeler D, Usdin K. The roles of Sp1, Sp3, USF1/USF2 and NRF-1 in the regulation and three-dimensional structure of the Fragile X mental retardation gene promoter. Vol. 386, Biochem. J. 2005.
39. Takahashi S, Sugimoto N. Watson-Crick versus Hoogsteen Base Pairs: Chemical Strategy to Encode and Express Genetic Information in Life. Acc Chem Res. 2021 May 4;54(9):2110–20.
40. Oumard A, Hennecke M, Hauser H, Nourbakhsh M. Translation of NRF mRNA Is Mediated by Highly Efficient Internal Ribosome Entry. Vol. 20. 2000.
41. Lee DSM, Ghanem LR, Barash Y. Integrative analysis reveals RNA G-quadruplexes in UTRs are selectively constrained and enriched for functional associations. Nat Commun. 2020 Dec 1;11(1).
42. Otovat F, Bozorgmehr MR, Mahmoudi A, Morsali A. Porphyrin-based ligand interaction with G-quadruplex: Metal cation effects. Journal of Molecular Recognition. 2023 Aug 1;36(8).
43. Balaratnam S, Torrey ZR, Calabrese DR, Banco MT, Yazdani K, Liang X, et al. Investigating the NRAS 5′ UTR as a target for small molecules. Cell Chem Biol. 2023 Jun 15;30(6):643-657.e8.

 doi:10.20944/preprints202601.1129.v1

44. Lee SC, Zhang J, Strom J, Yang D, Dinh TN, Kappeler K, et al. G-Quadruplex in the NRF2 mRNA 5′ Untranslated Region Regulates De Novo NRF2 Protein Translation under Oxidative Stress . Mol Cell Biol. 2017 Jan 1;37(1).
45. Wu S, Jiang L, Lei L, Fu C, Huang J, Hu Y, et al. Crosstalk between G-quadruplex and ROS. Vol. 14, Cell Death and Disease. Springer Nature; 2023.
46. Zang H, Mathew RO, Cui T. The Dark Side of Nrf2 in the Heart. Vol. 11, Frontiers in Physiology. Frontiers Media S.A.; 2020.
47. Brüschweiler S, Fuchs JE, Bader G, McConnell DB, Konrat R, Mayer M. A Step toward NRF2-DNA Interaction Inhibitors by Fragment-Based NMR Methods. ChemMedChem. 2021 Dec 6;16(23):3576–87.
48. Poganik JR, Long MJC, Disare MT, Liu X, Chang SH, Hla T, et al. Post-transcriptional regulation of Nrf2-mRNA by the mRNA-binding proteins HuR and AUF1. FASEB Journal. 2019 Dec 1;33(12):14636–52.
49. Kim YS, Kimball SR, Piskounova E, Begley TJ, Hempel N. Stress response regulation of mRNA translation: Implications for antioxidant enzyme expression in cancer. Vol. 121, Proceedings of the National Academy of Sciences of the United States of America. 2024.
50. Akl MG, Li L, Baccetto R, Phanse S, Zhang Q, Trites MJ, et al. Complementary gene regulation by NRF1 and NRF2 protects against hepatic cholesterol overload. Cell Rep. 2023 Apr 25;42(4).
51. Tebay LE, Robertson H, Durant ST, Vitale SR, Penning TM, Dinkova-Kostova AT, et al. Mechanisms of activation of the transcription factor Nrf2 by redox stressors, nutrient cues, and energy status and the pathways through which it attenuates degenerative disease. Vol. 88, Free Radical Biology and Medicine. Elsevier Inc.; 2015. p. 108–46.
52. Neupane A, Chariker JH, Rouchka EC. Structural and Functional Classification of G-Quadruplex Families within the Human Genome. Genes (Basel). 2023 Mar 1;14(3).
53. Miskiewicz J, Sarzynska J, Szachniuk M. How bioinformatics resources work with G4 RNAs. Vol. 22, Briefings in Bioinformatics. Oxford University Press; 2021.
54. Cagirici HB, Budak H, Sen TZ. G4Boost: a machine learning-based tool for quadruplex identification and stability prediction. BMC Bioinformatics. 2022 Dec 1;23(1).
55. Kikin O, D'Antonio L, Bagga PS. QGRS Mapper: A web-based server for predicting G-quadruplexes in nucleotide sequences. Nucleic Acids Res. 2006 Jul;34(WEB. SERV. ISS.).
56. Brázda V, Kolomazník J, Lýsek J, Bartas M, Fojta M, Šťastný J, et al. G4Hunter web application: A web server for G-quadruplex prediction. Bioinformatics. 2019 Sep 15;35(18):3493–5.
57. Javadekar SM, Nilavar NM, Paranjape A, Das K, Raghavan SC. Characterization of G-quadruplex antibody reveals differential specificity for G4 DNA forms. DNA Research. 2020 Oct 1;27(5).
58. Lago S, Nadai M, Rossetto M, Richter SN. Surface Plasmon Resonance kinetic analysis of the interaction between G-quadruplex nucleic acids and an anti-G-quadruplex monoclonal antibody. Biochim Biophys Acta Gen Subj. 2018 Jun 1;1862(6):1276–82.
59. Hellman LM, Fried MG. Electrophoretic mobility shift assay (EMSA) for detecting protein-nucleic acid interactions. Nat Protoc. 2007 Aug;2(8):1849–61.
60. Hou Y, Gan T, Fang T, Zhao Y, Luo Q, Liu X, et al. G-quadruplex inducer/stabilizer pyridostatin targets SUB1 to promote cytotoxicity of a transplatinum complex. Nucleic Acids Res. 2022 Apr 8;50(6):3070–82.
61. Rocca R, Talarico C, Moraca F, Costa G, Romeo I, Ortuso F, et al. Molecular recognition of a carboxy pyridostatin toward G-quadruplex structures: Why does it prefer RNA? Chem Biol Drug Des. 2017 Nov 1;90(5):919–25.
62. Liu LY, Ma TZ, Zeng YL, Liu W, Mao ZW. Structural Basis of Pyridostatin and Its Derivatives Specifically Binding to G-Quadruplexes. J Am Chem Soc. 2022 Jul 6;144(26):11878–87.
63. Zhang X, Spiegel J, Martínez Cuesta S, Adhikari S, Balasubramanian S. Chemical profiling of DNA G-quadruplex-interacting proteins in live cells. Nat Chem. 2021 Jul 1;13(7):626–33.
64. Seo M, Lei L, Egli M. Label-Free Electrophoretic Mobility Shift Assay (EMSA) for Measuring Dissociation Constants of Protein-RNA Complexes. Curr Protoc Nucleic Acid Chem. 2019 Mar 1;76(1).
65. Heffler MA, Walters RD, Kugel JF. Using electrophoretic mobility shift assays to measure equilibrium dissociation constants: GAL4-p53 binding DNA as a model system. Biochemistry and Molecular Biology Education. 2012 Nov;40(6):383–7.

 doi:10.20944/preprints202601.1129.v1

66. Sato K, Akiyama M, Sakakibara Y. RNA secondary structure prediction using deep learning with thermodynamic integration. Nat Commun. 2021 Dec 1;12(1).
67. Horspool DR, Coope RJ, Holt RA. Efficient assembly of very short oligonucleotides using T4 DNA Ligase. BMC Res Notes. 2010;3.
68. Fuller$ CW, Richardson CC. Initiation of DNA Replication at the Primary Origin of Bacteriophage T7 by Purified Proteins SITE AND DIRECTION OF INITIAL DNA SYNTHESIS*. Vol. 260, THE JOURNAL OF BIOLOGICAL CHEMISTRY. 1985.
69. Porecha R, Herschlag D. RNA radiolabeling. In: Methods in Enzymology. Academic Press Inc.; 2013. p. 255–79.
70. Yu L, Verwilst P, Shim I, Zhao YQ, Zhou Y, Kim JS. Fluorescent visualization of nucleolar g-quadruplex rna and dynamics of cytoplasm and intranuclear viscosity. CCS Chemistry. 2021;3(11):2725–39.
71. Dell'Oca MC, Quadri R, Bernini GM, Menin L, Grasso L, Rondelli D, et al. Spotlight on G-Quadruplexes: From Structure and Modulation to Physiological and Pathological Roles. Vol. 25, International Journal of Molecular Sciences. Multidisciplinary Digital Publishing Institute (MDPI); 2024.
72. Liu LY, Ma TZ, Zeng YL, Liu W, Mao ZW. Structural Basis of Pyridostatin and Its Derivatives Specifically Binding to G-Quadruplexes. J Am Chem Soc. 2022 Jul 6;144(26):11878–87.
73. Mei Y, Deng Z, Vladimirova O, Gulve N, Johnson FB, Drosopoulos WC, et al. TERRA G-quadruplex RNA interaction with TRF2 GAR domain is required for telomere integrity. Sci Rep. 2021 Dec 1;11(1).
74. Hashimoto Y, Kubo H, Kawauchi K, Miyoshi D. NRAS DNA G-quadruplex-targeting molecules for sequence-selective enzyme inhibition. Chemical Communications. 2024 Sep 27;
75. Hu XX, Wang SQ, Gan SQ, Liu L, Zhong MQ, Jia MH, et al. A Small Ligand That Selectively Binds to the G-quadruplex at the Human Vascular Endothelial Growth Factor Internal Ribosomal Entry Site and Represses the Translation. Front Chem. 2021 Nov 9;9.
76. Rouleau SG, Garant JM, Bolduc F, Bisaillon M, Perreault JP. G-Quadruplexes influence pri-microRNA processing. RNA Biol. 2018 Feb 1;15(2):198–206.
77. Jayaraj GG, Pandey S, Scaria V, Maiti S. Potential G-quadruplexes in the human long non-coding transcriptome. RNA Biol. 2012;9(1):81–9.
78. Dumas L, Herviou P, Dassi E, Cammas A, Millevoi S. G-Quadruplexes in RNA Biology: Recent Advances and Future Directions. Vol. 46, Trends in Biochemical Sciences. Elsevier Ltd.; 2021. p. 270–83.
79. Shu H, Zhang R, Xiao K, Yang J, Sun X. G-Quadruplex-Binding Proteins: Promising Targets for Drug Design. Vol. 12, Biomolecules. MDPI; 2022.
80. Cammas A, Desprairies A, Dassi E, Millevoi S. The shaping of mRNA translation plasticity by RNA G-quadruplexes in cancer progression and therapy resistance. Vol. 6, NAR Cancer. Oxford University Press; 2024.
81. Herdy B, Mayer C, Varshney D, Marsico G, Murat P, Taylor C, et al. Analysis of NRAS RNA G-quadruplex binding proteins reveals DDX3X as a novel interactor of cellular G-quadruplex containing transcripts. Nucleic Acids Res. 2018 Nov 30;46(21):11592–604.
82. Wu S, Jiang L, Lei L, Fu C, Huang J, Hu Y, et al. Crosstalk between G-quadruplex and ROS. Vol. 14, Cell Death and Disease. Springer Nature; 2023.
83. Kharel P, Ivanov P. RNA G-quadruplexes and stress: emerging mechanisms and functions. Vol. 34, Trends in Cell Biology. Elsevier Ltd.; 2024. p. 771–84.
84. Weng HY, Huang HL, Zhao PP, Zhou H, Qu LH. Translational repression of cyclin D3 by a stable G-quadruplex in its 5′ UTR: Implications for cell cycle regulation. RNA Biol. 2012;9(8):1099–109.
85. Van Drie JH, Tong L. Cryo-EM as a powerful tool for drug discovery. Vol. 30, Bioorganic and Medicinal Chemistry Letters. Elsevier Ltd.; 2020.
86. Kumari S, Bugaut A, Huppert JL, Balasubramanian S. An RNA G-quadruplex in the 5′ UTR of the NRAS proto-oncogene modulates translation. Nat Chem Biol. 2007;3(4):218–21.
87. Morris MJ, Basu S. An unusually stable G-quadruplex within the 5′-UTR of the MT3 matrix metalloproteinase mRNA represses translation in eukaryotic cells. Biochemistry. 2009 Jun 16;48(23):5313–9.

 doi:10.20944/preprints202601.1129.v1

88. Morris MJ, Negishi Y, Pazsint C, Schonhoft JD, Basu S. An RNA G-quadruplex is essential for cap-independent translation initiation in human VEGF IRES. J Am Chem Soc. 2010 Dec 22;132(50):17831–9.
89. Koukouraki P, Doxakis E. Constitutive translation of human a-synuclein is mediated by the 50-untranslated region. Open Biol. 2016 Apr 1;6(4).
90. Leppek K, Das R, Barna M. Functional 5′ UTR mRNA structures in eukaryotic translation regulation and how to find them. Vol. 19, Nature Reviews Molecular Cell Biology. Nature Publishing Group; 2018. p. 158–74.
91. Lee SC, Zhang J, Strom J, Yang D, Dinh TN, Kappeler K, et al. G-Quadruplex in the NRF2 mRNA 5′ Untranslated Region Regulates De Novo NRF2 Protein Translation under Oxidative Stress . Mol Cell Biol. 2017 Jan 1;37(1).
92. Dhyani N, Tian C, Gao L, Rudebush TL, Zucker IH. Nrf2-Keap1 in Cardiovascular Disease: Which Is the Cart and Which the Horse? Vol. 39, Physiology (Bethesda, Md.). 2024. p. 0.
93. Marion D. An introduction to biological NMR spectroscopy. Vol. 12, Molecular and Cellular Proteomics. 2013. p. 3006–25.
94. Kusi-Appauh N, Ralph SF, van Oijen AM, Spenkelink LM. Understanding G-Quadruplex Biology and Stability Using Single-Molecule Techniques. Vol. 127, Journal of Physical Chemistry B. American Chemical Society; 2023. p. 5521–40.
95. Thakur RK, Kumar P, Halder K, Verma A, Kar A, Parent JL, et al. Metastases suppressor NM23-H2 interaction with G-quadruplex DNA within c-MYC promoter nuclease hypersensitive element induces c-MYC expression. Nucleic Acids Res. 2009;37(1):172–83.
96. Kamzeeva PN, Alferova VA, Korshun VA, Varizhuk AM, Aralov A V. 5′-UTR G-Quadruplex-Mediated Translation Regulation in Eukaryotes: Current Understanding and Methodological Challenges. Int J Mol Sci [Internet]. 2025 Jan 30;26(3). Available from: http://www.ncbi.nlm.nih.gov/pubmed/39940956
97. Qi Q, Liu X, Xiong W, Zhang K, Shen W, Zhang Y, et al. Reducing CRISPR-Cas9 off-target effects by optically controlled chemical modifications of guide RNA. Cell Chem Biol. 2024 Oct 17;31(10):1839–51.
98. Yoneyama M, Kikuchi M, Natsukawa T, Shinobu N, Imaizumi T, Miyagishi M, et al. The RNA helicase RIG-I has an essential function in double-stranded RNA-induced innate antiviral responses. Nat Immunol. 2004 Jul;5(7):730–7.
99. Roy S, Ali A, Bhattacharya S. Theoretical Insight into the Library Screening Approach for Binding of Intermolecular G-Quadruplex RNA and Small Molecules through Docking and Molecular Dynamics Simulation Studies. Journal of Physical Chemistry B. 2021 Jun 3;125(21):5489–501.
100. Dickerhoff J, Warnecke KR, Wang K, Deng N, Yang D. Evaluating molecular docking software for small molecule binding to G-quadruplex DNA. Int J Mol Sci. 2021 Oct 1;22(19).
101. Prestwood PR, Yang M, Lewis G V., Balaratnam S, Yazdani K, Schneekloth JS. Competitive Microarray Screening Reveals Functional Ligands for the DHX15 RNA G-Quadruplex. ACS Med Chem Lett. 2024 Jun 13;15(6):814–21.
102. Wu G, Tillo D, Ray S, Chang TC, Schneekloth JS, Vinson C, et al. Custom G4 microarrays reveal selective G-quadruplex recognition of small molecule BMVC: A large-scale assessment of ligand binding selectivity. Molecules. 2020 Aug 1;25(15).
103. Castillo-González D, Pérez-Machado G, Pallardó F, Garrigues-Pelufo TM, Cabrera-Pérez MA. Send Orders of Reprints at reprints@benthamscience.net Computational Tools in the Discovery of New G-Quadruplex Ligands with Potential Anticancer Activity. Vol. 12, Current Topics in Medicinal Chemistry. 2012.
104. McPherson A, Cudney B. Optimization of crystallization conditions for biological macromolecules. Acta Crystallogr F Struct Biol Commun. 2014 Nov 1;70:1445–67.
105. Yadav DK, Lukavsky PJ. NMR solution structure determination of large RNA-protein complexes. Vol. 97, Progress in Nuclear Magnetic Resonance Spectroscopy. Elsevier B.V.; 2016. p. 57–81.
106. Maleki P, Budhathoki JB, Roy WA, Balci H. A practical guide to studying G-quadruplex structures using single-molecule FRET. Vol. 292, Molecular Genetics and Genomics. Springer Verlag; 2017. p. 483–98.
107. Masson T, Guetta CL, Laigre E, Cucchiarini A, Duchambon P, Teulade-Fichou MP, et al. BrdU immuno-tagged G-quadruplex ligands: a new ligand-guided immunofluorescence approach for tracking G-quadruplexes in cells. Nucleic Acids Res. 2021 Dec 16;49(22):12644–60.

 doi:10.20944/preprints202601.1129.v1

108. Meiser N, Fuks C, Hengesbach M. Cooperative analysis of structural dynamics in RNA-protein complexes by single-molecule Förster resonance energy transfer spectroscopy. Molecules. 2020 May 1;25(9).
109. Geraets JA, Pothula KR, Schröder GF. Integrating cryo-EM and NMR data. Vol. 61, Current Opinion in Structural Biology. Elsevier Ltd.; 2020. p. 173–81.
110. Monsen RC, Trent JO. G-quadruplex virtual drug screening: A review. Vol. 152, Biochimie. Elsevier B.V.; 2018. p. 134–48.
111. Schock Vaiani J, Broekgaarden M, Coll JL, Sancey L, Busser B. In vivo vectorization and delivery systems for gene therapies and RNA-based therapeutics in oncology. Nanoscale. Royal Society of Chemistry; 2025.
112. Birrer MJ, Moore KN, Betella I, Bates RC. Antibody-Drug Conjugate-Based Therapeutics: State of the Science. J Natl Cancer Inst. 2019 Jun 1;111(6):538–49.
113. Biffi G, Di Antonio M, Tannahill D, Balasubramanian S. Visualization and selective chemical targeting of RNA G-quadruplex structures in the cytoplasm of human cells. Nat Chem. 2014 Jan;6(1):75–80.
114. Luo L, Jea JDY, Wang Y, Chao PW, Yen L. Control of mammalian gene expression by modulation of polyA signal cleavage at 5′ UTR. Nat Biotechnol. 2024 Sep 1;42(9):1454–66.
115. Stevens AJ, de Jong L, Kennedy MA. The Dynamic Regulation of G-Quadruplex DNA Structures by Cytosine Methylation. Vol. 23, International Journal of Molecular Sciences. MDPI; 2022.
116. Vorlíčková M, Kejnovská I, Sagi J, Renčiuk D, Bednářová K, Motlová J, et al. Circular dichroism and guanine quadruplexes. Vol. 57, Methods. 2012. p. 64–75.
117. Wu S, Jiang L, Lei L, Fu C, Huang J, Hu Y, et al. Crosstalk between G-quadruplex and ROS. Vol. 14, Cell Death and Disease. Springer Nature; 2023.
118. Zou M, Li JY, Zhang MJ, Li JH, Huang JT, You PD, et al. G-quadruplex binder pyridostatin as an effective multi-target ZIKV inhibitor. Int J Biol Macromol. 2021 Nov 1;190:178–88.
119. Rodriguez R, Miller KM, Forment J V., Bradshaw CR, Nikan M, Britton S, et al. Small-molecule-induced DNA damage identifies alternative DNA structures in human genes. Nat Chem Biol. 2012;8(3):301–10.
120. Peng R, Huang Q, Wang L, Qiao G, Huang X, Jiang J, et al. G-quadruplex RNA Based PROTAC Enables Targeted Degradation of RNA Binding Protein FMRP for Tumor Immunotherapy. Angewandte Chemie International Edition. 2024 Nov 18;
121. Zhai LY, Liu JF, Zhao JJ, Su AM, Xi XG, Hou XM. Targeting the RNA G-Quadruplex and Protein Interactome for Antiviral Therapy. Vol. 65, Journal of Medicinal Chemistry. American Chemical Society; 2022. p. 10161–82.
122. Virgilio A, Amato T, Petraccone L, Esposito F, Grandi N, Tramontano E, et al. Improvement of the activity of the anti-HIV-1 integrase aptamer T30175 by introducing a modified thymidine into the loops. Sci Rep. 2018 Dec 1;8(1).
123. Esposito V, Pirone L, Mayol L, Pedone E, Virgilio A, Galeone A. Exploring the binding of d(GGGT)4 to the HIV-1 integrase: An approach to investigate G-quadruplex aptamer/target protein interactions. Biochimie. 2016 Aug 1;127:19–22.
124. Patil KM, Chin D, Seah HL, Shi Q, Lim KW, Phan AT. G4-PROTAC: Targeted degradation of a G-quadruplex binding protein. Chemical Communications. 2021 Dec 11;57(95):12816–9.